AUCTORES
Globalize your Research

Journal of Clinical Case Reports and Studies
Yuanmei Che *

Open Access

Research Article

m6A Demethylase FTO Contributes to Tuberculous Meningitis by Upregulating MMP-9 and OX-42 in Cortical Neurons

Xiaopeng Li [#], Li Gao [#], Lunli Zhang, Yuanbin Zhong, Liang Wang, Yuanmei Che*[#]

Department of Infection, First Affiliated Hospital of Nanchang University, Nanchang, Jiangxi Province, China.

* These authors contribute equally to this work

***Corresponding Author:** Yuanmei Che Department of Infection, First Affiliated Hospital of Nanchang University, Nanchang, Jiangxi Province, China.

Received date: September 10, 2025; **Accepted date:** October 08, 2025; **Published date:** October 15, 2025

Citation: Xiaopeng Li, Li Gao, Lunli Zhang, Yuanbin Zhong, Liang Wang, et al, (2025), m6A Demethylase FTO Contributes to Tuberculous Meningitis by Upregulating MMP-9 and OX-42 in Cortical Neurons**,** *J, Clinical Case Reports and Studies*, 6(7); **DOI**:10.31579/2690-8808/272

Abstract

FTO is an RNA N6-methyladenosine (m6A) demethylase. Despite the involvement of FTO in various neural diseases, its role in Tuberculosis meningitis (TBM) remains unclear.

Based on a high-throughput analysis, we found that FTO is transcriptionally activated in patients with TBM. We then validated that Tuberculous induced the expression of FTO in isolated mouse microglia and in mouse brain, which further increased the expression of matrix Metalloproteinase-9 (MMP-9) and Integrin alpha-M (ITGAM, or OX42). Knockdown of FTO dramatically abrogates the up-regulation of MMP-9 and OX42. FTO depletion also restores the Tuberculous -induced microglial apoptosis. We further validated that increased FTO can reduce m6A modifications in MMP-9 and OX42 transcripts.

Collectively, we showed that FTO contributes to TBM via up-regulating the expression of MMP-9 and OX42, indicating the potential therapeutic mechanisms of FTO in TBM.

Key Words: tuberculous meningitis, microglia, fto, mmp-9, ox-42

Introduction

Tuberculosis (TB) remains a threat to public health globally, which was the top cause of death from a single pathogen in the pre-COVID-19 era [1]. When aerosols that contain Mycobacterium tuberculosis (M.tb) enter the alveoli of the human lung, TB first develops as a pulmonary disease. Among extrapulmonary tuberculosis that occurs secondary to pulmonary TB, Tuberculosis meningitis (TBM) is the most severe disease. Its mortality is estimated to be in a range from 20% to 50%. For those who survive TBM, nearly half develop serious neural sequelae [2]. Yet, the molecular mechanisms underlying the pathogenesis of TBM remains elusive.

Matrix metalloproteinases (MMPs) are a superfamily of evolutionarily conserved protease that degrade the extracellular matrix (ECM) in a calcium- and zinc- dependent manner [3] [4]. Previous studies suggested that several MMPs were aberrantly up-regulated in TBM, indicating their involvement in TBM development. So far, human TBM researches mainly focused on the subfamily of gelatinases, MMP-2 (gelatinase-A) and MMP-9 (gelatinase-B) [5]. MMP-2 is constitutively expressed in the CNS whereas MMP-9 is kept silent or only expressed at a limited level under normal circumstances. However, MMP-9 is activated during neuroinflammation, typically in meningitis associated with bacterial infection [6]. In addition, increased level of MMP-9 in cerebrospinal fluid of TBM patients positively correlates with poor outcome [7-9]. Considering the biochemical role of gelatinase, highly expressed MMP-9 may participate in tissue destruction and blood-brain barrier (BBB) breakdown in TBM by degrading a wide range of ECM components, including type IV collagen, fibronectin, tenascins, proteoglycans and laminin [4, 5, 10]. Despite the potential pivotal roles of MMP-9 in TBM, how MMP-9 is regulated in TBM is unclear.

N6-methyladenosine (m6A) is the most prevalent and conserved modification in eukaryotic messenger RNA [11, 12]. Numerous studies have shown that m6A is critical for regulating the splicing, transport, localization and translation of mRNA in both physiological and pathological conditions (Roignant and Soller 2017, Yang, Hu et al. 2020). This epigenetic modification is a dynamic and reversible process. The m6A methyltransferase complex, or m6A writer, which comprises proteins methyltransferase-like 3 (METTL3), methyltransferase-like 14 (METTL14), and Wilms tumor 1 associated protein (WTAP) promotes m6A installation while demethylases such as obesity-associated protein (FTO) and AlkB homolog 5 (ALKBH5) assume the role of erasers to remove m6A marks [13, 14]. m6A modifications are recognized by m6A readers such as YTH-domain family 1-3 (YTHDF1-3) [15, 16]. The m6A demethylase FTO, or α-ketoglutarate-dependent dioxygenase, was shown to be associated with body mass index, thus predisposing to child and adult obesity [17]. Numerous studies have indicated that FTO can modulate a plethora of biological

processes including nutrient sensing, adipogenesis and mitochondrial biogenesis [18-20]. Although FTO is ubiquitously expressed in multiple tissues, it has a highest expression in the brain [21], suggesting its indispensable role in central neural system (CNS). FTO has been shown to be required for neural gene expression and thus neural development. It has been associated with many neuropsychiatric diseases, including Alzheimer's disease, Parkinson's disease, epilepsy, anxiety and depression [22, 23]. However, the role of FTO in CNS infectious disease has not been reported to the best of our knowledge so far.

In this study, the role of FTO in MBT was explored. First, the role of FTO in mouse primary microglia was studied. Microglia are macrophages residing in CNS that can recognize M.tb and are the main infected cells in CNS (Rock, Hu et al. 2005, Colonna and Butovsky 2017, Davis, Rohlwink et al. 2019). We report that FTO was upregulated upon TB inoculation in both cultured mouse microglia in vitro and brain in vivo and induced the expression of MMP-9 and OX-42. Our RNA immunoprecipitation experiment confirmed that MMP-9 and OX42 were demethylated in TB context. Overall, our study illuminated the promoting role of FTO in TBM. This indicates that FTO can be a potential therapeutic target for TBM.

Methods

RNA sequencing and data processing

Our study was approved by the Ethics Committee of the First Affiliated Hospital of Nanchang University. 3 ml of whole blood were collected from 15 TBM patients and 24 healthy volunteers. Total RNA was purified from whole blood using QIAamp RNA Blood Mini Kit (Qiagen, Germany). PolyA+ RNA was enriched from Total RNA using VAHTS DNA Clean Beads (Vazyme, China). Stranded mRNA library was constructed using VAHTS Universal V8 RNA-seq Library Prep Kit for Illumina (Vazyme, China). AMPure XP beads were used to purify to library. We then utilized 2100 Bioanalyzer (Agilent, USA) to examine the library size distribution. Library was quantified using Qubit Fluorometer (Thermo Fisher Scientific, USA) and Equalbit 1 × dsDNA HS Assay Kit (Vazyme, China). Sequencing was performed by Illumina Hiseq Platform PE150 (Illumina, USA).

Trimmomatic (v0.39) and TopHat (v2.1.1) were employed for sequence trimming and alignment respectively. The R package DESeq2 was used for both raw read normalization and differential gene expression. P values are adjusted based on Benjamini-Hochberg method. The genes with a false discovery rate (FDR) lower than 0.05 were considered differentially expressed.

Isolation, culture and transfection of mouse primary microglial cells

All animal experiments carried out in this study are in compliance with the National Institutes of Health Guide for the Care and Use of Laboratory Animals. Primary microglia cells were isolated from pathogen-free C57Bl/6 mouse pups. After decapitation, the mouse brains were dissected and kept in ice-cold Hank's buffered salt solution (HBSS), with the meninges stripped off. Then, we homogenized those brain tissues at 37°C in Dulbecco's modified Eagle's medium (DMEM), supplemented with 10% fetal bovine serum penicillin (50 U/mL), streptomycin (50 lg/mL), Fungizon (0.5 lg/mL), and L-glutamine (2 mM) (Invitrogen, USA). The cell suspension was centrifuged and the pellet was collected, followed by resuspension in fresh medium to remove debris. Cells from two brains were combined and seeded in one T-75 flask at 37 °C in a humidified incubator with 5% CO2. Medium was replaced by fresh medium every four days. After 11-12 days, we isolated the primary microglia cells from the monolayer of astrocytes by agitation. Immunohistochemical approaches were used to assess the purity of isolated microglial cells (95%). Plasmids for cell transfection were synthesized by Gemma Gene (Shanghai, China). The short hairpin RNA (shRNA) sequences are shown as follows. sh-FTO: 5'-AAGGACGTTCCCAATAGCCAA-3'; Scrambled non-targeting RNA: 5'-UUCUCCGAACGUGUCACGUTT-3'. Cells were seeded in a six-well plate and transfection was performed using Lipofectamine 2000 (Invitrogen, USA) in accordance with the manufacturer's instructions when the confluence reaches 70%.

M. tuberculosis maintenance and infection

M. tuberculosis H37Rv strain was cultivated at 37°C in Middlebrook 7H9 liquid broth (Difco, USA) that contains oleic acid-albumin dextrose catalase (ADC), 0.05% Tween 80 and 0.5% glycerol. One day prior to infection, primary microglial cells were plated in 6-well plates (Falcon, USA) at 2.5×105 cells per well. Cells were then infected with diluted M. tuberculosis H37Rv. The approximate infection ratio is 10 bacilli per microglial cell. To establish murine TB model, we anesthetized mice with isoflurane. 1×105 cfu of H37Rv (based on counts on M7H11 agar plates) in 50 μL of saline was then injected intracerebrally, as descried previously [24].

Cell transfection & in vivo knockdown

Plasmids for cell transfection were synthesized by Gemma Gene (Shanghai, China). The short hairpin RNA (shRNA) sequences are shown as follows. sh-FTO: 5'-AAGGACGTTCCCAATAGCCAA-3'; scrambled non-targeting RNA: 5'-UUCUCCGAACGUGUCACGUTT-3'. Cells were seeded in a six-well plate and transfection was performed using Lipofectamine 2000 (Invitrogen, USA) in accordance with the manufacturer's instructions when the confluence reaches 70%. For in vivo knockdown, we expressed sh-FTO and the scramble shRNA using a lentivirus vector under the control of U6 promoter. Lenti-Pac HIV Expression Packaging Kit (GeneCopoeia, USA) was used for Lentivirus production. Cortical injection of high-titer lentivirus preparation was performed 24 h after H37Rv infection, directed by a stereotaxic apparatus.

Western blotting

Cells were lysed using lysis buffer with the supernatant collected for further immunoblotting experiments. Before the assay, the concentration of protein was measured using BCA kit (Epizyme, China). Equivalent proteins were then loaded into 10 % SDS-PAGE gels. Separated proteins were then transferred to polyvinylidene difluoride (PVDF) membranes. Membranes were incubated using in tris-buffered saline containing 0.1 % Triton X-100 (TBST) with 5% nonfat milk for 1 h. After blocking, membranes were incubated by primary antibody diluted in TBST overnight at 4 ℃. Concentrations of each antibody used in this study were listed as follows: anti-FTO (1:1,500, Abcam, UK); anti-MMP-9 (1:1,000, Abcam, UK); anti-OX-42 (1:1,000, Invitrogen, USA); anti-METTL14 (1:1,500, Invitrogen, USA); anti-GFAP (1:1,000, Cell Signaling Technology, USA); anti-β-Actin (1:1,000; Sigma, USA); anti-GAPDH (1:2,000, Invitrogen, USA).

Membranes were washed for 5 min using TBST for three times at room temperature. Appropriate secondary antibodies diluted in TBST were then added to those membranes, which were incubated for 1 h at room temperature. After washing in PBST for three times, images were taken for membranes treated with chemiluminescence reagent (Vazyme, China) immediately. All western blotting experiments were performed three times independently, with representative data shown in the figures. Densitometry analysis was conducted using ImageJ software [25].

TUNEL assay

Apoptotic microglial cells were detected by TUNEL assay. Mouse primary microglial cells were cultured and transfected with negative control or sh-FTO on coverslips. After transfection for 72h, cells were harvested and fixed with phosphate buffered saline (PBS) containing 4% formaldehyde (FA) for 20 min. Then cells were kept for 5 min in PBS with 0.2 % Triton X-100 for permeabilization. A TUNEL staining kit was used to stain apoptotic cells according to instructions provided by manufacturer (Abcam, UK). Cell nucleus were stained by PI (50 μg/ml). Slides were examined by Leica

DM3000 fluorescence microscopy (Leica, Germany). Images were taken by DFC 420 camera (Leica, Germany).

RNA isolation and quantitative RT-PCR (RT-qPCR)

Total RNA was isolated from cultured primary microglial cells using TRIzol reagent (Invitrogen, USA). Then the RNA was reverse transcribed to cDNA using a reverse transcription kit according to the protocol provided by manufacturer (Vazyme, China). To evaluate the relative mRNA levels, we performed quantitative PCR (qPCR) experiments using Real-time PCR kits (Yeasen, China). Primers used in qPCR were shown as follows: FTO (Forward 5'-CGGTATCTCGCATCCTCATT -3'; Reverse 5'-ATTTCAGCCTCGGTGTGTTT-3'); METTL14 (Forward: 5'-GAGCTGAGAGTGCGGATAGC-3'; Reverse: 5'-GCAGATGTATCATAGGAAGCCC-3'); MMP-9 (Forward: 5'-AGGACCGCTTCTACTGGCG-3'; Reverse: 5'-CTCCTCCCTTTCCTCCAGAAC-3'); ITGAM (OX42) (Forward: 5'-TTTCATGAGCCTGGACTGCC-3'; Reverse: 5'-TTCAAGGCCCCAGACACTTC-3').

Prediction of m6A sites

m6A sites of MMP-9 and ITGAM transcripts were predicted by SRAMP (sequence-based RNA adenosine methylation site predictor, http://www.cuilab.cn/sramp). Prediction was performed based on default setting.

Methylated RNA immunoprecipitation (MeRIP)

Total RNA was extracted from primary microglial cells using TRIzol (Invitrogen, USA) and treated by DNase I (Sigma Aldrich, USA). rRNA was removed using RiboMinus Eukaryote Kit (Invitrogen, USA). RNAs were then physically fragmented by sonication for 10 seconds on a mixture of ice and water. For MeRIP, RNA fragments were incubated with an anti-N6-methyladenosine antibody (1:1,000, Abcam, USA) or control IgG (1:1,000, Cell Signaling Technology, USA) conjugated to magnetic beads (Invitrogen, USA) in Magna RIP buffer (MilliporeSigma, USA) overnight at 4 °C. The beads were then incubated with Proteinase K for 1.5h at 42 °C. Phenol-chloroform extraction method was used to isolate RNAs. Methylated RNA levels were determined by RT-qPCR followed by agarose gel electrophoresis.

Statistical analysis

All values are presented as the means ± standard deviation. All experiments are performed three times independently. Statistical differences among groups were determined using unpaired Student's t-test. p values less than 0.05 were considered statistically significant. All statistical analyses in this study were performed by GraphPad Prism 7 software. All data presented in this article are available upon request.

Results

Transcriptomic aberrations by TBM suggested the dysregulation of m6A modifier

We first performed an RNA-seq for whole blood from TBM patients and healthy individuals. 907 differentially expressed genes (DEGs) were identified, including 340 up-regulated genes and 567 down-regulated genes (Figure 1A). Among those genes showed a dramatic expression change (fold change > 2 or < 0.5), DEGs were predominantly enriched in biological processes related to immune responses with an extremely low p value (adjusted p = 7.66×10-32). Apart from immune processes, metalloproteinase activities were also affected. 48 and 52 DEGs were enriched in GO term metalloendopeptidase activity and metallopeptidase activity with an adjusted p value of 2.28×10-31 and 1.83×10-21, respectively (Figure 1B). Interestingly, among those DEGs, we found that many genes involved in m6A modification were also differentially expressed in TBM patient (Figure 1C). Several m6A writers WTAP, ZC3H3 and RBM15/15B were down-regulated while m6A readers such as IGF2BP2, IGF2BP3 and YTHDF3 were up-regulated. It was worth noticing that the eraser FTO was upregulated (adjusted p = 3.53×10-7, log2FC = 0.74) while ALKBH5 remain unchanged (adjusted p = 0.08). Since multiple m6A writers and readers were dysregulated, the sole differential expression of FTO may indicated the unique role of FTO in TBM.

TB induced ectopic FTO expression in mouse primary microglial cells

To investigate the non-redundant role of FTO, we examined its expression in mouse primary microglial cells infected by M.tb. After being co-cultured with H37Rv, a strain of M.tb, for 12 hours, the microglia showed a dramatic increase of FTO level while Mettl14 was not affected (Figure 2A&B), consistent with our RNA-seq data. Unexpectedly, the expression of FTO was notably down-regulated 24 hours post-infection (hpi) compared to 12 hpi (Figure 2 B). This indicated that the FTO induction by TB might be transient and dynamic. We then questioned whether FTO was up-regulated in microglial cells transcriptionally or post-transcriptionally. Quantitative reverse transcription PCR (RT-qPCR) results suggested a much higher transcript abundance of FTO in 12 hpi group compared to both control and 24 hpi group (Figure 3A, consistent to our immunoblotting data. Similarly, Mettl14 was transcriptionally unchanged during TB (Figure 3B). This result implies that RNA demethylation, rather than RNA methylation, was involved in TBM.

TB led to an FTO-dependent upregulation of MMP-9, Ox-42 and GFAP

Based on this finding, we further explored the consequences of ectopic FTO expression in CNS when infected with M.tb. OX-42, also known as CD11b encoded by ITGAM, a marker for activated macrophage was first examined [26-29]. The expression of OX-42 was significantly up-regulated upon TB for 12 h, indicating microglial activation. Similarly, the expression level of Glial fibrillary acid protein (GFAP), a molecular marker for astroglia was also higher than the non-infected group. More importantly, when FTO was depleted by RNAi in TB-infected microglial cells, the expression level of OX-42 and GFAP was restored ($p < 0.05$, Figure 3A and B upper left). Apart from those two microglial markers, we wondered whether TB-induced FTO also controlled MMP-9, a gelatinase with potential engagement in TBM. As shown in Figure 3 A and B, infected microglia showed a much higher level of MMP-9, and this up-regulation was dramatically mitigated upon FTO knockdown ($p < 0.01$). These results suggested that TB-induced ectopic FTO promoted the expression of OX-42, GFAP and MMP-9.

FTO contributed to apoptosis triggered by TB

The elevated level of MMP-9 may lead to a loss of collagen, which may further promote cell death [30]. Thus, we asked if cell death was also regulated by FTO in the context of TB. TdT-mediated dUTP-biotin nick end labeling (TUNEL) assay was performed to detect cell apoptosis of microglia cells. Inter-nucleosomal DNA fragmentation was stained to indicate cells that have undergone programmed cell death [31]. Apoptotic signals, as labelled red, in microglial cells infected with H37Rv were dramatically up-regulated compared to the control group while FTO depletion notably reduced the positive TUNEL signals (Figure 5A&B). The apoptosis rescued by FTO shRNA indicated that FTO was involved in the regulation of programmed cell death in TBM.

FTO mediates the upregulation of MMP-9 and OX-42 by TB in vivo

Since we have observed that FTO induced the expression of OX-42, GFAP and MMP-9 in primary microglial cells, we wondered if FTO was also required for their elevation in vivo. For the infection group, mouse brains were injected with H37Rv and analyzed after one month (1M). In accordance to the in vitro data, OX-42, GFAP and MMP were all up-regulated in 1M group, and FTO depletion partially restored their expression level in cortex neurons infected with H37Rv for one month (Figure 6 A&B). Consistently,

our in vivo experiment supported that FTO induced the expression of MMP-9, OX-42 and GFAP (Figure 6 A, C, D and E). Since OX-42 and GFAP are the indicative markers for microglia and astroglia respectively, this result might indicate that FTO can regulate the activation of microglia and astroglia.

TB induces the demethylation of OX-42 and MMP-9 transcripts

Considering the role of FTO in mRNA modification, we hypothesized that FTO controlled the expression of OX-42 and MMP-9 via directly demethylating their transcripts. To test this hypothesis, we first performed an in silico prediction of the m6A sites in those two transcripts using SCRAMP. It was shown that MMP-9 possessed 6 potential methylation sites, among which three sites are over moderate confidence. To experimentally verify this, we combined RNA immunoprecipitation (RIP) and RT-qPCR. The antibody that specifically recognizes m6A site was harnessed in our RNA immunoprecipitation assay to pulldown the transcripts with m6A modification. A control IgG was used as a control to confirm the antibody specificity. Then, those transcripts were reverse transcribed and amplified, which was subjected to electrophoresis for a final detection (Figure 7A). Primers was designed for a 241-bp amplicon in MMP-9 transcript that covers candidate site P5 (2139) and P6 (2225) (Figure 7B). By electrophoresis, the m6A modification in the transcript of MMP-9 was validated in cultured non-infected microglia with no amplified signal in the IgG-pulldown group. More importantly, when infected with M.tb for 12h, the level significantly reduced, suggesting an enhanced demethylation by up-regulated FTO. The same approach that combines bioinformatic analysis and RIP/RT-qPCR was used to detect the m6A modification of OX-42 as well (Figure 8A). Analysis by SRAMP discovered 9 out of 12 potential methylation sites over moderate confidence in the transcript of OX-42. Based on this, we amplified a fragment that allows a simultaneous detection for any m6A modification of 4 candidate sites (P7-P10, i.e., 2364, 2459, 2503 and 2525) (Figure 8B). Similarly, m6A modification was found in RNAs pulled down by m6A-specific antibodies and this level was reduced 12 hpi (Figure 8C). Those data demonstrated that MMP-9 and OX-42 were post-transcriptionally regulated by m6A modification, and m6A level declined upon TB, coinciding with the up-regulation of FTO. Taken together, our results suggested that TB induced the expression of MMP-9 and OX-42 in an FTO-dependent manner.

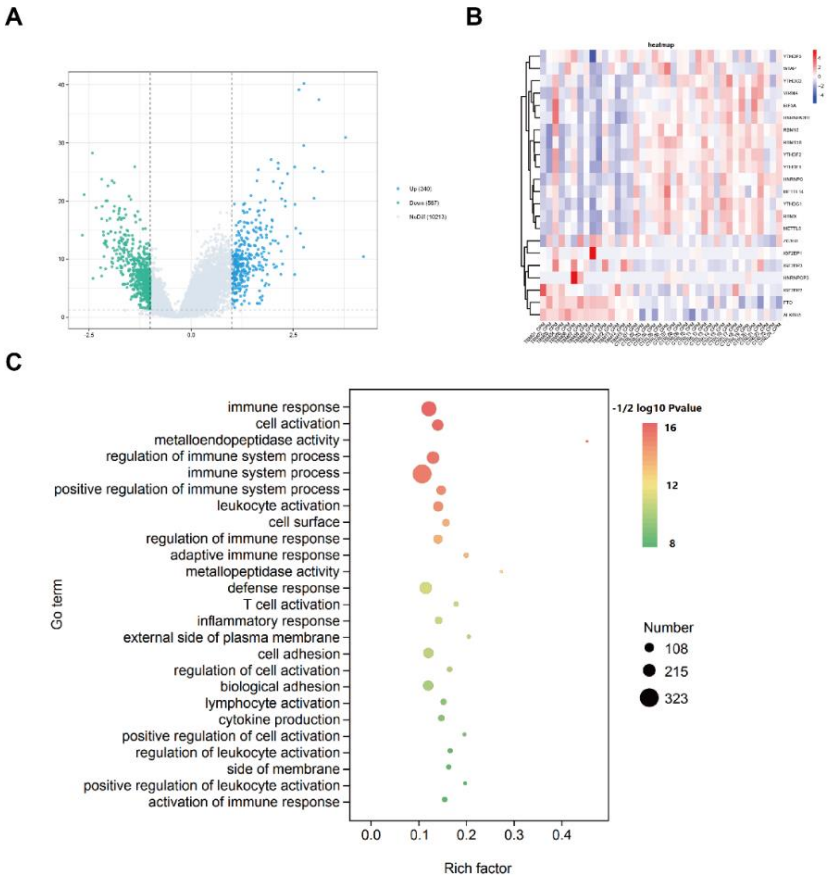

Figure 1: Transcriptional profile alterations induced by TBM.

A. Volcano plot depicting all differentially expressed genes (DEGs)

B. Heatmap showing the expression of genes involved in m6A modification

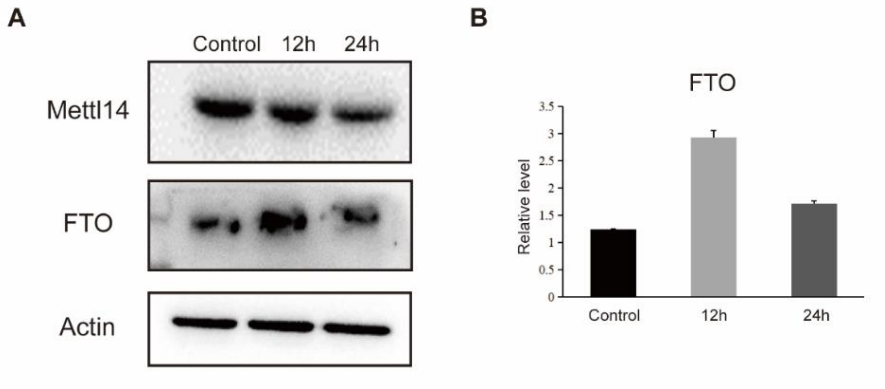

Figure 2: The expression of FTO and METTL14 in M.tb infected and non-infected mouse primary microglial cells

A. Representative Western blots of FTO and METTL14 in mouse primary microglia co-cultured with H37Rv for 12h or 24h.
B. Associated quantitative analysis of FTO and METTL14. *p < 0.05 versus non-infected (Control) group; #p < 0.05 versus 12h group.

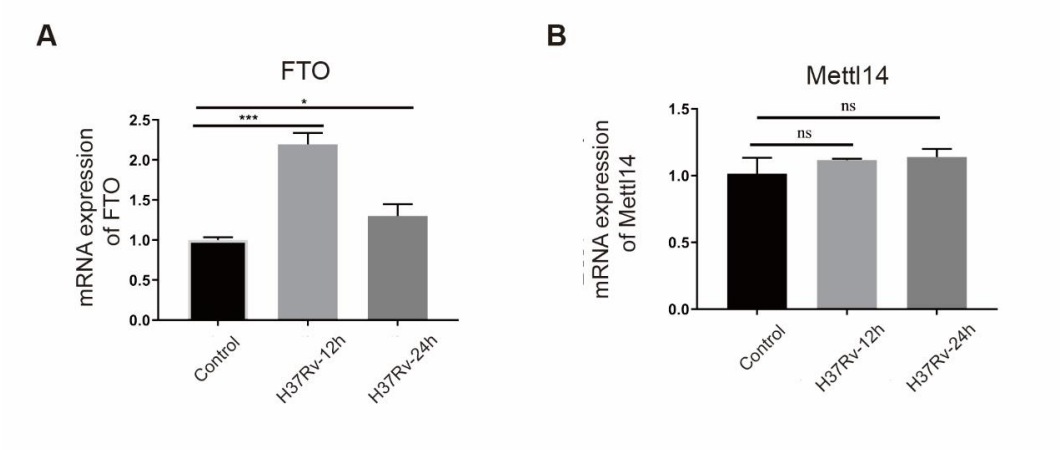

Figure 3: TB alters the transcriptional profile of FTO in mouse primary microglia

A. mRNA level of METTL14 is not affected upon M.tb infection.

B. mRNA level of FTO is increased in microglia infected by M.tb after 12h and 24h. *p < 0.05 versus non-infected control group; ***p < 0.01 versus the control group.

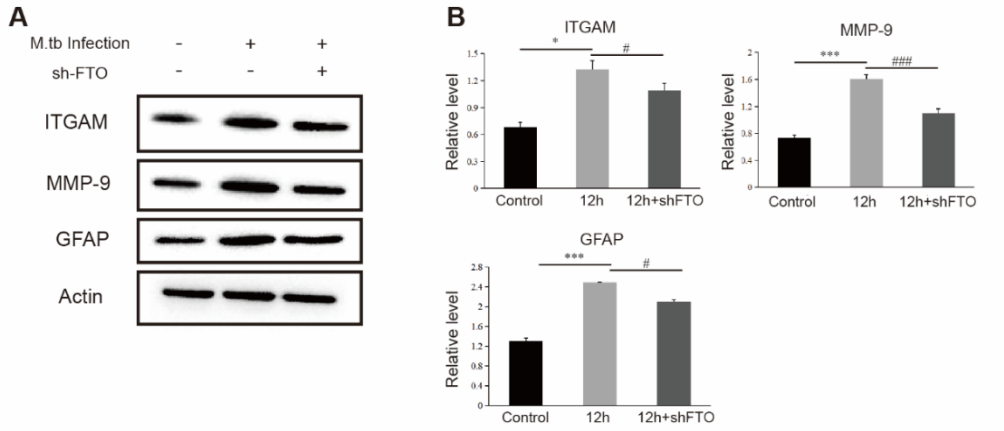

Figure 4: FTO is required for the up-regulation of ITGAM, MMP-9, and GFAP in primary microglia by TB.

A. Representative Western blots of OX-42, MMP-9 and GFAP in non-infected (Control), 12h-infection (12h) and 12h-infection microglia transfected with sh-FTO (12h+sh-FTO). Actin was used as an internal control.

B. Associated quantification. *p < 0.05 versus control group; ***p < 0.01 versus 12 h-infection group; #p < 0.05 versus control group; ###p < 0.05 versus control group.

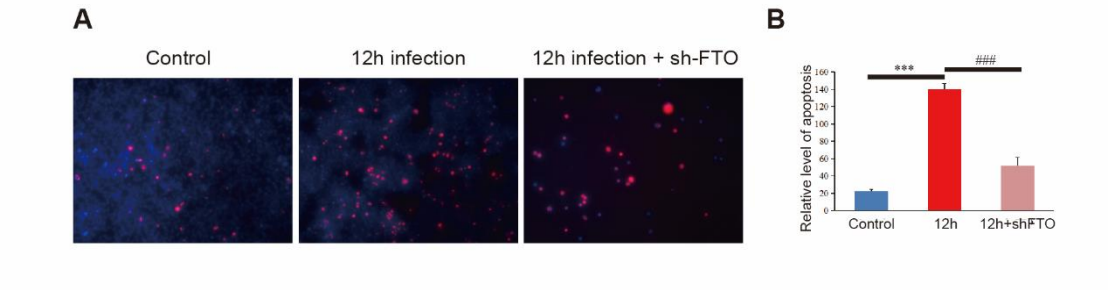

Figure 5: FTO is required for microglial apoptosis caused by TB.

A. TUNEL assay of microglial cell in control, 12h and 12h+sh-FTO group. Nuclei is shown in blue while positive TUNEL signals that indicate apoptosis are in red.

B. Quantification of apoptotic cell number. ***p < 0.01 versus control group; ###p < 0.01 versus microglial cell treated with H37Rv for 12h.

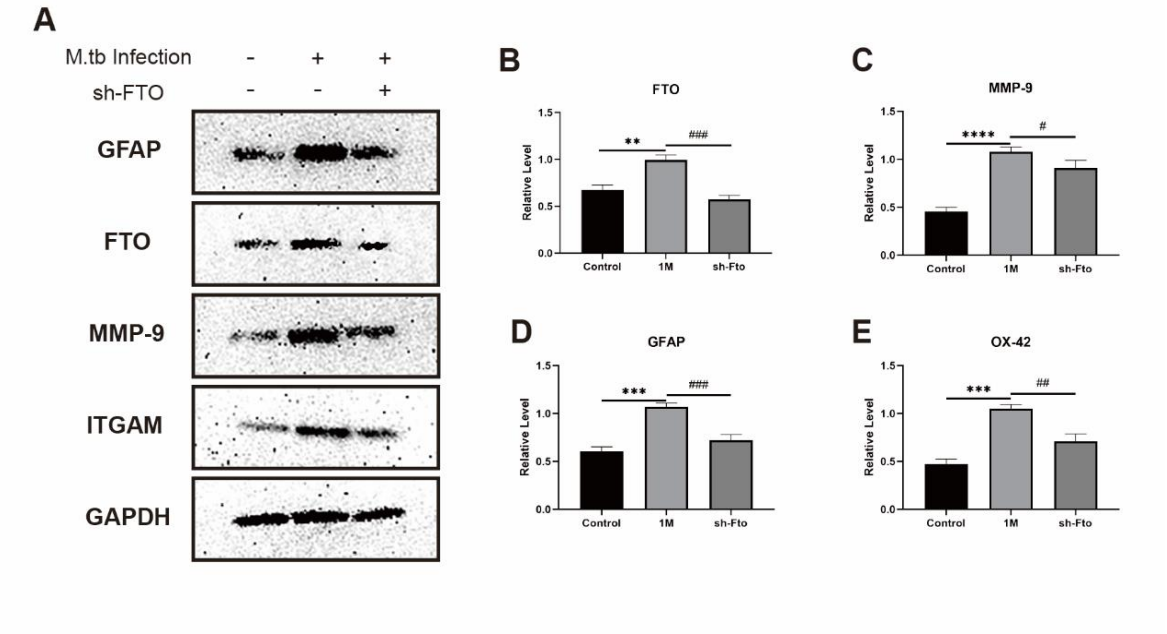

Figure 6: FTO positively regulates MMP-9, OX-42 and GFAP in vivo

A. Representative immunoblots of FTO, OX-42, MMP-9 and GFAP in mouse cortex neuron from uninfected individuals (Ctrl), individuals infected with M.tb for a month (1M) and individuals infected for a month with FTO knockdown (1M+shFTO). GAPDH was used as an internal control.

B. Densitometry analysis of FTO. ** p < 0.01 versus control group; ### p < 0.001 versus 1M group.

C. Densitometry analysis of MMP-9. **** p < 0.0001 versus control group; # p < 0.05 versus 1M group.

D. Densitometry analysis of GFAP. *** p < 0.001 versus control group; ### p < 0.001 versus 1M group.

E. Densitometry analysis of OX-42. *** p < 0.001 versus control group; ## p < 0.01 versus 1M group.

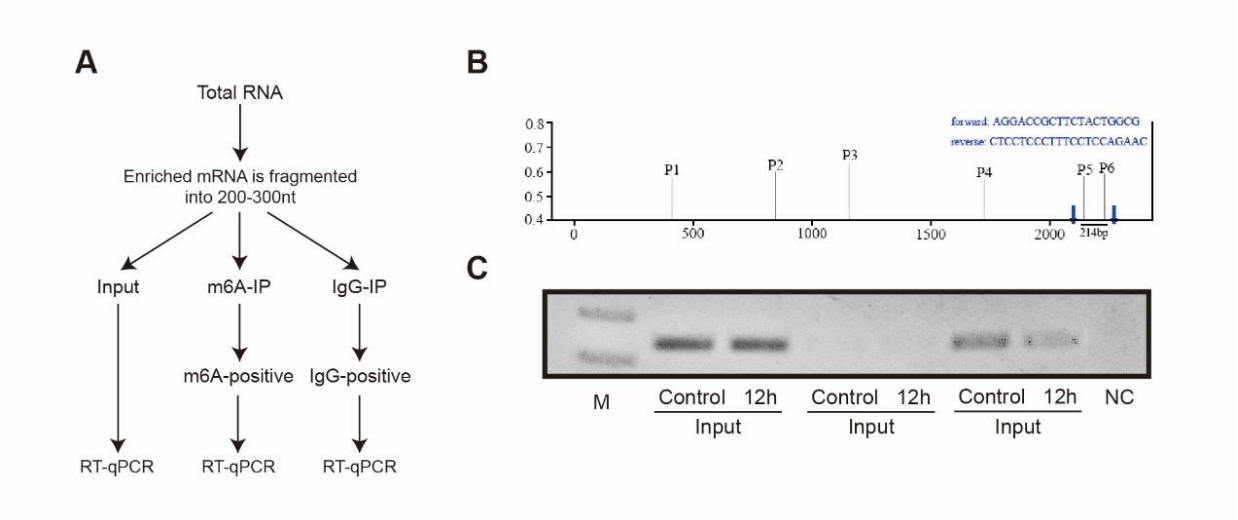

Figure 7: The mRNA of MMP-9 is demethylated in M.tb-infected microglial cells.

A. Schematic diagram showing the detecting workflow for MMP-9 transcripts.

B. Predicted m6A sites and target fragment amplified using indicated primers on MMP-9 mRNA transcripts.

C. Target fragment amplified from MMP-9 transcripts pulled down by indicated antibodies from normal (Control) and primary microglia infected with M.tb for 12h (12h), examined by agarose gel electrophoresis. M: ladder marker; NC: negative control (no reverse transcription template).

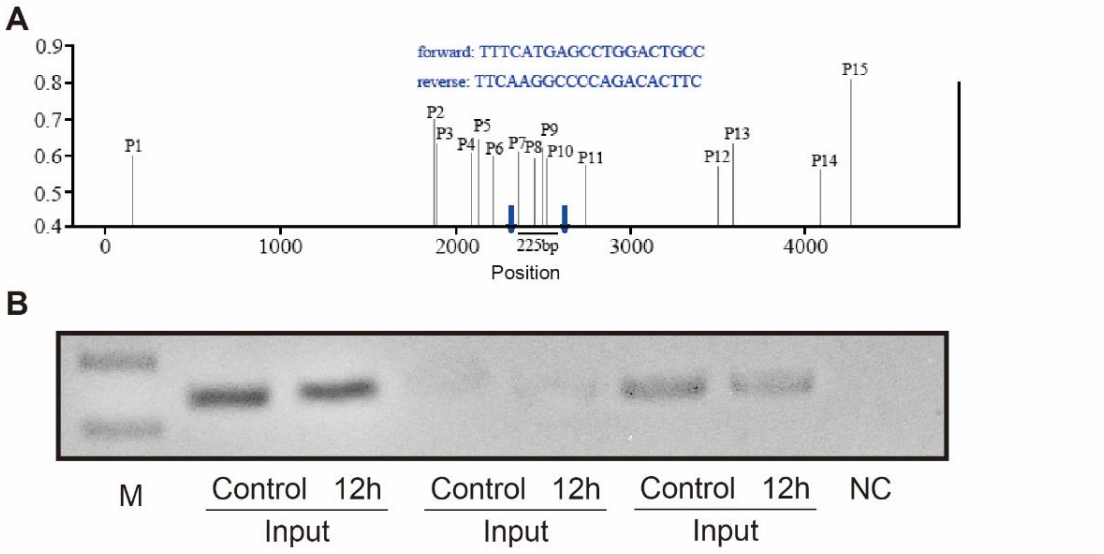

Figure 8: The mRNA of OX-42 is demethylated in M.tb-infected microglial cells.

A. Predicted m6A sites and target fragment amplified using indicated primers on OX-42 mRNA transcripts.

B. Target fragment amplified from MMP-9 transcripts pulled down by indicated antibodies from normal (Control) and primary microglia infected with M.tb for 12h (12h), examined by agarose gel electrophoresis. M: ladder marker. NC: negative control (no template control).

Discussion

The main treatment strategy for MBT is antibiotic therapy based on the strategy for pulmonary TB. Yet, due to the limited penetration of BBB, the drug level in cerebrospinal fluid (CSF) may be insufficient with no standard for optimal drug dosage and combination established so far. For antibiotic-resistant TBM, few effective therapeutic approaches have been reported, which is normally led to extremely poor outcome [32]. The lack of therapeutic strategy may be largely attributed to the insufficient understanding of the molecular mechanism underlying TBM pathogenesis. Therefore, in-depth study of TBM is important for therapy development. Here, we verified the involvement of m6A in TBM progression, providing novel insights into TBM pathogenesis.

Physiologically, the expression of MMP-9 is limited in CNS. Clinal studies establish that the abnormally high concentration of MMP-9 in CSF of TBM patients is associated to TBM severity, including tissue damage and neurological compromise [9, 33]. Host-directed drug that specifically targets

MMP-9 may provide a solution adjunctive with conventional antibacterial therapy. The MMP-9-specific inhibitor SB-3CT was shown to enhance TB bacilli clearing while BBB disruption was also ameliorated for TBM rats treated with another MMP inhibitor, Batimastat (BB-94) [34, 35]. Although MMP-9 plays a vital role in TBM and has been studies clinically and pharmaceutically, how MMP-9 is up-regulated in TBM remains largely unknown. Our study identifies FTO as the positive regulator of MMP-9. This is supported by our data that MMP-9 is upregulated during TB and that FTO RNAi reversed the elevation of MMP-9 (Figure 4 and Figure 6). Furthermore, RNA immunoprecipitation experiments validated the m6A modification in MMP-9 transcript, which are directly controlled by FTO (Figure 7).

m6A is a common RNA modification, playing a multifaceted role in mRNA modulation. It is estimated that m6A occurs in approximately 30% transcripts [36]. Due to the universality of m6A, it regulates the expression of a myriad of genes, thereby exerting important functions physiologically. Thus, m6A disruption may lead to aberrant gene expression, which further causes the dysregulation of cellular functions. It is widely believed that m6A is involved in many diseases, such as cancers, psychiatric disorders, osteoporosis, and metabolic disease [36]. However, only a few studies link m6A with infectious disease. For instance, m6A-modified viral transcripts are less likely to bind to cytosolic RIG-I-like receptors to trigger antiviral signaling [37]. It is also demonstrated that m6A regulators participate in other immunoregulatory processes, including inflammatory response and autoimmune [38, 39]. However, little is known about the role of m6A in bacterial infectious diseases. This is the first study that establishes the link between m6A and bacterial infection.

Herein, robust evidences are provided to support that the m6A demethylase FTO (but not the methyltransferase Mettl14) is involved in TBM. We first showed that TB induces the ectopic expression of FTO in both cultured microglial cells (Figure 2 and Figure 3) and in vivo (Figure 6), and then functionally validated the engagement of FTO in TB-induced apoptosis (Figure 5). Intriguingly, FTO is shown to be a positive regulator of apoptosis in the context of TBM, which is a founding contradictory to the majority of previous studies. FTO is considered as an apoptotic inhibitor since its overexpression inhibits apoptosis while its knockdown promotes cell death. This apoptotic-inhibiting role is confirmed in a wide range of contexts, including adipocytes, multiple cancer cells and myocardial cells with hypoxia/reoxygenation injury [40-43]. By contrast, the pro-apoptotic function is much less frequently reported, limited to only a few cancer types such as clear cell renal cell carcinoma and intrahepatic cholangiocarcinoma [44, 45]. These contradictory results suggest that FTO plays a dual role in apoptosis modulation, which is likely to be transcriptional context-dependent. Our data also highlighted that TB altered the epigenetic landscape of the transcripts of MMP-9 and OX42 by inducing the ectopic expression of m6A eraser FTO. The uninstallation of m6A then stabilizes the mRNA of MMP-9 and OX-42, ultimately leading to their upregulation. Considering the role of MMP-9, FTO may be a potential therapeutic target for TBM. Upon inhibition of FTO, the MMP-9 down-regulation may at least partially restore the BBB integrity and alleviate CNS tissue destruction. Actually, MMP-9 is not the only known MMP controlled by FTO, a study in 2020 found that FTO was also overexpressed in esophageal squamous cell carcinoma and it contributes to the up-regulation of MMP13 [46]. We speculate that the transcripts of other MMPs may also harbor m6A modification sites, which were also regulated by FTO, and that FTO-dependent MMP regulation may be implicated in diseases beyond cancer and TBM.

Apart from MMP-9, we also found the m6A sites in the mRNA of OX42 (integrin subunit alpha M or ITGAM). Similar to MMP-9, our data suggest that TB promoted the demethylation and stabilization of OX-42 transcript, causing the upregulation of OX-42. OX-42 is a component of complement receptor 3, a critical molecule in pro-inflammatory responses [47], which normally remains expressed at a low level in the CNS [48]. Genome-wide association study (GWAS) data unveiled the genetic association between OX-42 and several autoimmune diseases, such as systemic lupus erythematosus, scleroderma and multiple sclerosis [29, 49, 50]. By genotyping patients with common variable immunodeficiency disorders, Maggadottir et al. found that multiple signaling pathways of B and T cell are enriched in OX-42-interacting network [51]. Although these hypothesis-free GWAS studies established OX-42 as a risk factor of autoimmune diseases and identified the risk alleles based on single nucleotide polymorphisms (SNPs), it is still unknown how these SNPs affect the expression of OX-42. Furthermore, functional research into OX-42 is sparse [52]. Thus, it still remains a question how OX-42 is regulated in vivo and whether OX-42 is involved and dysregulated in other diseases. Our data not only illuminated the abnormal elevation of OX-42 in CNS infected by M.tb (Figure 4 and Figure 6), but also mechanically demonstrated that this upregulation is mediated by m6A demethylation FTO (Figure 8). This finding suggests that the role of OX-42 may be more diverse than we expected, at least not limited in autoimmunity.

Taken together, our study shed light on the involvement of m6A modification in TBM, and the removal of m6A in the transcripts of MMP-9 and OX42 led to their stabilization, which may further functionally contribute to the development of TBM. Our study deepened the current understanding of TBM pathogenesis and more importantly, provided new insights into the development of non-antibiotic therapy of TBM.

Reference

1. Chakaya, J., et al., (2021). Global Tuberculosis Report 2020–Reflections on the Global TB burden, treatment and prevention efforts. International Journal of Infectious Diseases, 113: p. S7-S12.
2. Graham, S.M. and P.R. Donald, (2014). Death and disability: the outcomes of tuberculous meningitis. The Lancet Infectious Diseases, 14(10): p. 902-904.
3. Löffek, S., O. Schilling, and C.-W. Franzke, (2011). Biological role of matrix metalloproteinases: a critical balance. *European Respiratory Journal*, 38(1): p. 191-208.
4. Rosenberg, G.A., Matrix metalloproteinases in neuroinflammation. Glia, 2002. 39(3): p. 279-291.
5. Rohlwink, U.K., et al., (2019). Matrix metalloproteinases in pulmonary and central nervous system tuberculosis—a review. International journal of molecular sciences, 20(6): p. 1350.
6. Leppert, D., et al., (2000). Matrix metalloproteinase (MMP)-8 and MMP-9 in cerebrospinal fluid during bacterial meningitis: association with blood-brain barrier damage and neurological sequelae. Clinical Infectious Diseases, 31(1): p. 80-84.
7. Majeed, S., et al., (2016). role of matrix metalloproteinase− 9 in progression of tuberculous meningitis: a pilot study in patients at different stages of the disease. BMC Infectious diseases, 16(1): p. 1-7.
8. Matsuura, E., et al., (2000). Marked increase of matrix metalloproteinase 9 in cerebrospinal fluid of patients with fungal or tuberculous meningoencephalitis. Journal of the neurological sciences, 173(1): p. 45-52.
9. Price, N.M., et al., (2001). Identification of a matrix-degrading phenotype in human tuberculosis in vitro and in vivo. The Journal of Immunology, 166(6): p. 4223-4230.
10. Lee, K.Y., et al., (2004). Persistent increase of matrix metalloproteinases in cerebrospinal fluid of tuberculous meningitis. Journal of the neurological sciences, 220(1-2): p. 73-78.
11. Fu, Y., et al., (2014). Gene expression regulation mediated through reversible m6A RNA methylation. Nature Reviews Genetics, 15(5): p. 293-306.

12. Jiang, X., et al., (2021). The role of m6A modification in the biological functions and diseases. Signal transduction and targeted therapy, 6(1): p. 1-16.
13. Roundtree, I.A., et al., (2017). Dynamic RNA modifications in gene expression regulation. Cell, 169(7): p. 1187-1200.
14. Zhang, C., J. Fu, and Y. Zhou, (2019). A Review in Research Progress Concerning m6A Methylation and Immunoregulation. Frontiers in Immunology, 10.
15. Patil, D.P., B.F. Pickering, and S.R. Jaffrey, (2018). Reading m6A in the transcriptome: m6A-binding proteins. Trends in cell biology, 28(2): p. 113-127.
16. Lasman, L., et al., (2020). Context-dependent functional compensation between Ythdf m6A reader proteins. Genes & development, 34(19-20): p. 1373-1391.
17. Frayling, T.M., et al., (2007). A common variant in the FTO gene is associated with body mass index and predisposes to childhood and adult obesity. Science, 316(5826): p. 889-894.
18. Fawcett, K.A. and I. Barroso, (2010). The genetics of obesity: FTO leads the way. Trends in genetics, 26(6): p. 266-274.
19. Wang, X., et al., (2017). FTO is required for myogenesis by positively regulating mTOR-PGC-1α pathway-mediated mitochondria biogenesis. Cell Death & Disease, 8(3): p. e2702-e2702.
20. Gulati, P., et al., (2013). Role for the obesity-related FTO gene in the cellular sensing of amino acids. Proceedings of the National Academy of Sciences, 110(7): p. 2557-2562.
21. Gerken, T., et al., (2007). The obesity-associated FTO gene encodes a 2-oxoglutarate-dependent nucleic acid demethylase. Science, 318(5855): p. 1469-1472.
22. Annapoorna, P., et al., (2019). FTO: an emerging molecular player in neuropsychiatric diseases. Neuroscience, 418: p. 15-24.
23. Yeo, G.S. and S. O'Rahilly, (2012). Uncovering the biology of FTO. Molecular metabolism, 1(1-2): p. 32-36.
24. Van Well, G.T.J., et al., (2007). A new murine model to study the pathogenesis of tuberculous meningitis. The *Journal of infectious diseases*, 195(5): p. 694-697.
25. Schneider, C.A., W.S. Rasband, and K.W. Eliceiri, (2012). NIH Image to ImageJ: 25 years of image analysis. Nature methods, 9(7): p. 671-675.
26. Benveniste, E.N., (1997). Role of macrophages/microglia in multiple sclerosis and experimental allergic encephalomyelitis. *Journal of molecular medicine*, 75(3): p. 165-173.
27. Rao, N.A., et al., (2003). Pathogenic Role of Retinal Microglia in Experimental Uveoretinitis. Investigative Opthalmology & Visual Science, 44(1): p. 22.
28. Matsumoto, Y., K. Ohmori, and M. Fujiwara, (1992). Microglial and astroglial reactions to inflammatory lesions of experimental autoimmune encephalomyelitis in the rat central nervous system. Journal of neuroimmunology, 37(1-2): p. 23-33.
29. Nath, S.K., et al., (2008). A nonsynonymous functional variant in integrin-α M (encoded by ITGAM) is associated with systemic lupus erythematosus. Nature genetics, 40(2): p. 152-154.
30. Al Shammari, B., et al., (2015). The extracellular matrix regulates granuloma necrosis in tuberculosis. The *Journal of infectious diseases*, 212(3): p. 463-473.
31. Loo, D.T., TUNEL Assay, in In Situ Detection of DNA Damage: Methods and Protocols, V.V. Didenko, Editor. 2002, Humana Press: Totowa, NJ. p. 21-30.
32. Wilkinson, R.J., et al., (2017). Tuberculous meningitis. Nature reviews neurology, 13(10): p. 581-598.
33. Harris, J.E., et al., (2007). Monocyte-astrocyte networks regulate matrix metalloproteinase gene expression and secretion in central nervous system tuberculosis in vitro and in vivo. The *Journal of Immunology*, 178(2): p. 1199-1207.
34. Paul, R., et al., (1998). Matrix metalloproteinases contribute to the blood—brain barrier disruption during bacterial meningitis. Annals of Neurology: Official Journal of the American Neurological Association and the Child Neurology Society, 44(4): p. 592-600.
35. Majeed, S., B.D. Radotra, and S. Sharma, (2016). Adjunctive role of MMP-9 inhibition along with conventional anti-tubercular drugs against experimental tuberculous meningitis. *International Journal of Experimental Pathology*, 97(3): p. 230-237.
36. Yang, C., et al., (2020). The role of m6A modification in physiology and disease. Cell death & disease, 11(11): p. 1-16.
37. Durbin, A.F., et al., (2016). RNAs containing modified nucleotides fail to trigger RIG-I conformational changes for innate immune signaling. MBio, 7(5): p. e00833-16.
38. Rubio, R.M., et al., (2018). RNA m6 A modification enzymes shape innate responses to DNA by regulating interferon β. Genes & development, 32(23-24): p. 1472-1484.
39. Liu, J., et al., (2019). CCR7 chemokine receptor-inducible lnc-Dpf3 restrains dendritic cell migration by inhibiting HIF-1α-mediated glycolysis. Immunity, 50(3): p. 600-615. e15.
40. Shen, Z., et al., (2021). FTO inhibits UPRmt-induced apoptosis by activating JAK2/STAT3 pathway and reducing m6A level in adipocytes. Apoptosis, 26(7): p. 474-487.
41. Shen, W., et al., (2021). FTO overexpression inhibits apoptosis of hypoxia/reoxygenation-treated myocardial cells by regulating m6A modification of Mhrt. Molecular and Cellular Biochemistry, 476(5): p. 2171-2179.
42. Ke, W.-L., et al., (2022). m6A demethylase FTO regulates the apoptosis and inflammation of cardiomyocytes via YAP1 in ischemia-reperfusion injury. Bioengineered, 13(3): p. 5443-5452.
43. Wang, J.-y., L.-j. Chen, and P. Qiang, (2020). The potential role of N6-methyladenosine (m6A) demethylase fat mass and obesity-associated gene (FTO) in human cancers. OncoTargets and therapy, 13: p. 12845.
44. Zhuang, C., et al., (2019). N6-methyladenosine demethylase FTO suppresses clear cell renal cell carcinoma through a novel FTO-PGC-1α signalling axis. Journal of cellular and molecular medicine, 23(3): p. 2163-2173.
45. Rong, Z.-X., et al., (2019). Downregulation of fat mass and obesity associated (FTO) promotes the progression of intrahepatic cholangiocarcinoma. Frontiers in oncology, 9: p. 369.
46. Liu, S., et al., (2020). FTO promotes cell proliferation and migration in esophageal squamous cell carcinoma through up-regulation of MMP13. Experimental Cell Research, 389(1): p. 111894.
47. Kienzler, A., C. Hargreaves, and S. Patel, (2017). The role of genomics in common variable immunodeficiency disorders. Clinical & Experimental Immunology, 188(3): p. 326-332.
48. Fagerberg, L., et al., (2014). Analysis of the human tissue-specific expression by genome-wide integration of transcriptomics and antibody-based proteomics. Molecular & cellular proteomics, 13(2): p. 397-406.
49. Fagerholm, S., et al., (2013). The CD11b-integrin (ITGAM) and systemic lupus erythematosus. Lupus, 22(7): p. 657-663.

50. Anaya, J.-M., et al., (2012). Evaluation of genetic association between an ITGAM non-synonymous SNP (rs1143679) and multiple autoimmune diseases. Autoimmunity reviews, 11(4): p. 276-280.
51. Maggadottir, S.M., et al., (2015). Rare variants at 16p11. 2 are associated with common variable immunodeficiency. *Journal of Allergy and Clinical Immunology*, 135(6): p. 1569-1577.
52. Zhang, Y.-M., X.-J. Zhou, and H. Zhang, (2017). What genetics tells us about the pathogenesis of IgA nephropathy: the role of immune factors and infection. Kidney international reports, 2(3): p. 318-331.

DOI:10.31579/2690-8808/275